Local geometry of Fe^{3+} ions on the potassium sites in $KTaO_3$

H. Donnerberg and M. Exner
University of Osnabrück, Postbox 4469, D-4500 Osnabrück, Germany

C. R. A. Catlow
The Royal Institution of Great Britain, Davy Faraday Research Laboratory, 21 Albemarle Street, London W1X 4BS, Great Britain
(Received 1 July 1992)

We present the results of our computer-simulation study on the Fe^{3+} incorporation in $KTaO_3$. We find that Fe^{3+} ions enter the crystal lattice by means of a self-compensation-type reaction, i.e., by creation of Fe_K^{3+} and Fe_{Ta}^{3+} substitutional defects. Moreover, an energetically feasible model reaction is suggested for the occurrence of both axial defect centers Fe_{Ta}^{3+}-V_O and Fe_K^{3+}-O_I. Finally, a superposition-model analysis, based on a Lennard-Jones-type radial $\bar{b}_2$ function, shows that the ground-state axial zero-field splitting parameter of $D=4.46\ cm^{-1}$, found experimentally, should be explained by Fe_K^{3+}-O_I. This result, supported by shell-model calculations, contradicts a prior superposition-model analysis.

I. INTRODUCTION

Cubic potassium tantalate, an ideal perovskite, is a convenient material to study the incorporation of extrinsic defects without the complications of nonstoichiometry (as in $LiNbO_3$ for example), phase transitions, or high intrinsic defect concentrations. The results obtained for this compound may possibly aid the understanding of defect structures in other crystals, e.g., potassium niobate or potassium niobate-tantalate, which are very promising materials for electro-optical and photorefractive applications. Iron related defects are believed to play a central role in the photorefractive effect in many materials.

Electron paramagnetic resonance (EPR) experiments have shown that the Fe^{3+} ion can reside on both cation sites in $KTaO_3$. In addition to cubic type spectra,[1] which are assigned to the dopant ion substituting for both cations with remote charge compensation, axial type spectra are observed. These usually are ascribed to Fe_{Ta}^{3+}-V_O and Fe_K^{3+}-O_I, V_O being an oxygen vacancy and O_I an oxygen ion on the nearest interstitial site to the Fe_K^{3+}.[2]

The ground-state axial zero-field splitting parameter D is measured as $1.33\ cm^{-1}$ for the Ta site axial center and $4.46\ cm^{-1}$ for the K site axial center [2]. The Ta site axial D parameter is in line with former results for Fe^{3+}-V_O in other perovskite crystals.[3]

Zhou Yi-Yang[4] claims that a superposition model analysis can explain the large D parameter in the case of Fe_K^{3+} without invoking O_I. Instead he assumes a pronounced off-center displacement of the Fe^{3+} ion combined with a considerable inward relaxation of the oxygen ligands of about 0.3 Å. No reason is given as to why some of the Fe^{3+} ions remain at the K site, as is definitively proven by EPR,[1] whereas others should relax considerably. In addition the possible existence of a nearby interstitial oxygen has been discarded from further discussion because of its presumed negative contribution to the D value.

In a recent Comment[5] it was stated that an oxygen interstitial in the vicinity of the Fe^{3+} defect is compatible with the large D parameter if the oxygen ligands relax slightly further in the direction of the z axis in order to outweigh the presumed negative contribution of the oxygen interstitial. However, we believe that the assumption of such large inward oxygen relaxations (>0.3 Å) is physically not very plausible on ion size arguments and should therefore be ruled out from explanations of the large D parameter. After a careful reexamination of the propositions made by Zhou Yi-Yang we turn back to the idea of a nearby oxygen interstitial ion.

In Sec. II of this paper we present shell model calculations on iron related defects in $KTaO_3$. These allow us to derive definite conclusions concerning the defect chemistry of the iron incorporation as well as information on defect-induced lattice relaxations. This is ensued by a superposition model analysis in Sec. III, which we perform in the light of these shell model calculation results. We show that a $[Fe_K^{3+}-O_I]$ defect complex readily explains the large value of D, which was measured for the K site substitution of Fe^{3+}.

II. SHELL-MODEL RESULTS

In the shell model[6] each ion consists of a charged core to which a charged shell is coupled harmonically, allowing electronic polarization effects to be taken into account. In addition to long-range Coulomb potentials between different ions, short-range potentials of the Buckingham form, i.e., the sum of a repulsive Born-Mayer potential and a dispersive van der Waals term are specified between pairs of ion shells. The latter potentials are parametrized either theoretically using Hartree-Fock or electron gas techniques or empirically by a least-squares fitting to experimental data of the material under investigation. For defect calculations a two-region strategy is applied. The energy of the system is minimized both for the perfect and the defect lattice by independent displacement of the core and shell coordinates using a Newton-

Raphson minimization algorithm. The difference in the energy in the two cases is the defect energy. The method is coded in the CASCADE program, details of which are given in Ref. 7.

The short-range potential parameters used for the simulation of $KTaO_3$ (Table I) were fitted empirically to structural, elastic, and dielectric properties of the material. The parameters for the Fe^{3+}-O^{2-} interaction were also derived empirically.[8]

Here we only report those results concerning the incorporation of Fe^{3+} and the creation of oxygen interstitials and vacancies. For a general description of our simulation studies on $KTaO_3$ we refer to a forthcoming publication.[9] The basic results obtained in our study have been shown to be reasonably robust to variation of the shell-model parameters provided that these give a valid representation of the material.

The most favorable way for Fe^{3+} to enter $KTaO_3$ is by the following self-compensation reaction

$$Fe_2O_3 + \text{“}KTaO_3\text{”} \rightarrow Fe_K^{3+} + Fe_{Ta}^{3+} + KTaO_3 \ . \quad (1)$$

Reaction (1) is 3.36 eV more favorable than the competitive reaction (2) which is second lowest in energy:

$$Fe_2O_3 + \text{“}KTaO_3\text{”} \rightarrow 2Fe_K^{3+} + K_{Ta}^{+} + KTaO_3 \ . \quad (2)$$

Reaction (1) differs from reaction (2) only in that one Fe_{Ta}^{3+} ion and a K^+ ion are interchanged.

The incorporation of extrinsic ions via self-compensation has been seen to be of general importance in perovskite type crystals ABO_3, with cationic charge states A^+ and B^{5+}, e.g., $LiNbO_3$ and $KNbO_3$, though in the case of $LiNbO_3$ its occurrence is usually suppressed by intrinsic defects.[10] Moreover, for certain trivalent cations self-compensation is also known to occur in $BaTiO_3$,[8] in which the host cations are in the charge states A^{2+} and B^{4+}.

The question of how the Fe_K^{3+}-O_I center can be created or whether O_I can be present in the crystal arises, because in general O_I are found to be energetically unfavorable in oxide perovskites.

Oxygen Frenkel defect pairs are not likely to be present since their formation energy is 3.4 eV per defect. The reaction

$$Fe_2O_3 + \text{“}KTaO_3\text{”} \rightarrow 2Fe_K^{3+} + 2O_I^{2-} + K_2O \quad (3)$$

requires 16.10 eV more than the self-compensation reaction equation (1) and is therefore energetically unfeasible. Even when taking the binding energy of the complex

$$Fe_K^{3+} + O_I^{2-} \rightarrow [Fe_K^{3+}\text{-}O_I^{2-}] \quad (4)$$

of -3.53 eV into account the energy of (3) remains too high. It should be stressed that a charge compensation of Fe_K^{3+} by Fe_{Ta}^{3+} is much more favorable than by oxygen interstitials.

As a solution to the problem we suggest the following reaction, where self-compensation has been accepted as their main incorporation mechanism for Fe^{3+}:

$$Fe_K^{3+} + Fe_{Ta}^{3+} \rightarrow [Fe_K^{3+} - O_I^{2-}] + [Fe_{Ta}^{3+} - V_O] \ . \quad (5)$$

Here V_O denotes a doubly ionized oxygen vacancy. The energy for (5) is $+1.35$ eV per oxygen defect complex. This “induced oxygen Frenkel defect” type reaction reduces the energy to create oxygen interstitials by more than 2 eV compared to the simple oxygen Frenkel reaction. The energy is sufficiently low for appreciable concentrations of these species to be generated at high temperatures at which the crystals are grown. The trapped interstitials and vacancies will be immobile at low temperatures, hence their recombination is prevented.

Equation (5) also explains the simultaneous appearance of the centers $[Fe_K^{3+}\text{-}O_I^{2-}]$ and $[Fe_{Ta}^{3+}\text{-}V_O]$. By combining defect formation energies from shell-model calculations with the relevant ionization energies we find that the energy of the following charge transfer reaction (6) is $+0.58$ eV.

$$[Fe_K^{3+} - O_I^{2-}] \rightarrow [Fe_K^{2+} - O_I^{1-}] \ . \quad (6)$$

This shows that the defect center $[Fe_K^{3+}\text{-}O_I^{2-}]$ is stable with respect to the indicated charge redistribution. However, the small value of the energy for (6) indicates that pronounced covalency should be present at this defect center. The analogous center in $KNbO_3$ is unstable (-0.90 eV) in agreement with its absence in EPR measurements in $KNbO_3$.

It is important to note that the above results are valid for nonreduced $KTaO_3$ crystals. Usual growth conditions, however, imply some degree of reduction of the material.

$$\text{“Void”} \rightarrow V_O^{\cdot\cdot} + 2e' + \tfrac{1}{2}O_2 \ . \quad (7)$$

Here we adopt the Kröger-Vink notation and e' denotes

TABLE I. Potential parameters for $KTaO_3$ and Fe^{3+}.

	Core parameters[a]				Shell parameters[b]	
Interactions	A (eV)	ρ (Å)	C (eV Å^{-6})	Ion	Y/e	k (eV Å^{-2})
O^{2-}-O^{2-}	22764.3	0.149	27.627	O^{2-}	-2.75823	30.211
Ta^{5+}-O^{2-}	1315.572	0.36905	0.0	Ta^{5+}	-4.596	5916.770
K^+-O^{2-}	523.156	0.34356	0.0	K^+		
Fe^{3+}-O^{2-}	1102.4	0.3300	0.0	Fe^{3+}		

[a]Short-range interactions Buckingham function $A\exp(-r/\rho) - C/r^6$.

[b] Y=shell charge (the sum of core and shell charge yields the formal ionic charge of each ion); k=core-shell harmonic spring constant.

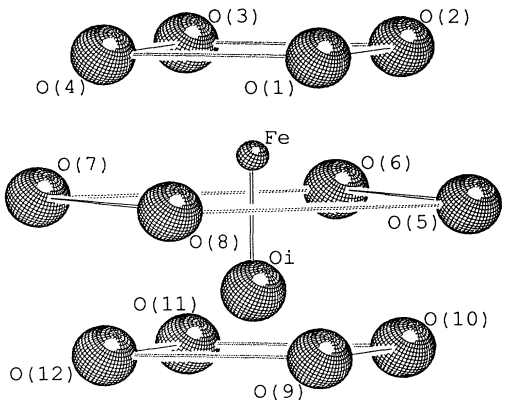

FIG. 1. $KTaO_3$: Fe_K^{3+}-O_I defect configuration. The defect is aligned on the z axis. O(1)-O(4): upper oxygen plane; O(5)-O(8): central oxygen plane; O(9)-O(12): lower oxygen plane; O_i: oxygen interstitial.

an electron. The energy for (7) is 6.7 eV. Oxygen vacancies may be trapped, possibly at the Fe_{Ta}^{3+} centers thereby providing another source for the observed Fe_{Ta}^{3+}-V_O centers. The electrons are trapped at low-lying electronic states in the gap, e.g., of Fe_K^{3+} centers. This reduces Fe^{3+} to Fe^{2+}. If no precautions are made to trap the electrons at other, lower defect states, the Fe_K^{3+} center becomes invisible in the EPR experiment. Experimentally the addition of Ti^{4+} ions[1] leads to observable Fe_K^{3+} and $[Fe_K^{3+}$-$O_I^{2-}]$ centers. Interestingly, shell-model calculations[9] show that Ti^{4+} is incorporated into $KTaO_3$ by a self-compensation type reaction. The existing Ti_K^{4+} defects provide electronic states which are energetically more attractive for electrons than the Fe_K^{3+} states. If no states are available in the gap, the electrons will be trapped at Ta sites, reducing Ta^{5+} to Ta^{4+}.

Shell-model calculations also allow us to obtain geometrical information on the local environment of a defect. In the case of the isolated Fe_K^{3+} the 12 oxygen ligands are displaced 0.29 Å towards the iron defect. The ligand-defect and nearest-neighbor ligand-ligand separation then is 2.53 Å. The Fe^{3+} ion remains almost exactly on the potassium site.

For the $[Fe_K^{3+}$-$O_I^{2-}]$ defect complex the calculations show that the oxygen interstitial moves 0.23 Å away from Fe_K^{3+} which in turn moves 0.40 Å towards the oxygen interstitial, thus leading to a reduction of the $[Fe_K^{3+}$-$O_I^{2-}]$ distance by about 0.2 Å. The relaxed separation of the two defects is 1.83 Å. Referring to the assignment of the planes as shown in Fig. 1, the oxygen ligands in the lower plane (close to O_I) relax outwards, whereas ligands in the upper plane (close to the Fe^{3+}) move ~ 0.33 Å in the direction of Fe^{3+} resulting in a Fe_K^{3+}-O^{2-} ligand separation of 2.1 Å. The distance of neighboring oxygen ions in the upper plane becomes 2.54 Å. Ligand ions in the central plane do not move significantly. In all cases discussed the magnitude of the oxygen relaxation is compatible with generally accepted values for ionic radii.

A list of coordinates is given in Table II. Because of the axial symmetry of the center, only one representative ligand ion for each plane needs to be specified.

III. SUPERPOSITION-MODEL RESULTS

The superposition model of Newman[11] allows us to interpret the experimentally determined ground-state axial zero-field splitting parameter D in terms of the local distortion of the environment of a paramagnetic defect center. The dependence of D on the polar coordinates R_i and θ_i of the n individual ligands i of the defect is given by the superposition formula

$$D=\sum_{i=1}^{n}\bar{b}_2(R_i)\tfrac{1}{2}[3\cos^2(\theta_i)-1]\ . \tag{8}$$

The z axis is chosen to coincide with the direction of the axial center and the origin is at the position of the defect. The radial function $\bar{b}_2(r)$ is the only input depending on the nature of the defect and of its ligand ions. Although until now it is in many cases impossible to obtain this function from first-principle *ab initio* calculations, it has become clear that positive as well as negative contributions of similar magnitude to $\bar{b}_2(r)$ have to be taken into account.[12] Empirically this finding can be expressed in using a Lennard-Jones-type formula for the radial dependence:[12,13]

$$\bar{b}_2(r)=A\left[\frac{R_0}{r}\right]^M+B\left[\frac{R_0}{r}\right]^N\ . \tag{9}$$

In most cases the reference distance R_0 is chosen as the perfect lattice spacing of the investigated cubic oxide. It should be noted that most published parameters for the

TABLE II. Coordinates from shell-model calculation for $[Fe_K^{3+}$-$O_I^{2-}]$ in $KTaO_3$ (coordinates and displacements are given in fractions of the lattice parameter $a=3.9885$ Å).

	Unrelaxed coordinates			Relaxed coordinates			Displacement
Species	x_0/a	y_0/a	z_0/a	x/a	y/a	z/a	d/a
Fe^{3+}	0.00000	0.00000	0.25000	0.00000	0.00000	0.14959	0.10041
O_I^{2-}	0.00000	0.00000	−0.25000	0.00000	0.00000	−0.30815	0.05815
O^{2-}	0.50000	0.00000	0.50000	0.44959	0.00000	0.43286	0.08396
O^{2-}	0.50000	0.50000	0.00000	0.50146	0.50146	−0.00970	0.00992
O^{2-}	0.50000	0.00000	−0.50000	0.61358	0.00000	−0.56632	0.13152

radial function refer to another expression

$$\bar{b}_2(r)=\bar{b}_2(R_0)\left[\frac{R_0}{r}\right]^{t_2}, \tag{10}$$

which can be taken as an approximation of Eq. (9) for r values close to the reference distance R_0. Uniaxial stress experiments on cubic oxides doped with the S-state ion under investigation have proven to be very useful in deriving the *a priori* unknown parameters in Eqs. (9) and (10).

Extensive work on Fe^{3+}-related $\bar{b}_2(r)$ parameters has been done by Müller and co-workers (e.g., Refs. 3 and 13). They discussed uniaxial stress experiments performed on MgO:Fe^{3+} and $SrTiO_3$:Fe^{3+}. They derived the following parameters for Eq. (9):

$$A=-0.68\ \text{cm}^{-1}\ ,\quad B=0.27\ \text{cm}^{-1}\ ,\quad M=10\ ,\quad N=13\ ,$$

and for Eq. (10):

$$\bar{b}_2(R_0)=-0.41\ \text{cm}^{-1}\ \text{and}\ t_2=8\ .$$

Both sets of parameters refer to $R_0=2.101$ Å. Figure 2 shows $\bar{b}_2(r)$ for these two parameter sets (solid curves). In particular it is noted that the Lennard-Jones-type formula (9) unambiguously yields a function, which has a minimum at $R_m<R_0$. For separations less than R_m, $\bar{b}_2(r)$ given by (9) increases for decreasing r values. Such a behavior also was concluded for Gd^{3+} and other rare earth ions.[12] In addition one may attempt to justify the Lennard-Jones-type $\bar{b}_2(r)$ dependence at smaller distances by LCAO-based approaches to the ground-state zero-field splitting EPR parameter D.[14,15] These investigations yield increasingly positive $\bar{b}_2(r)$ values, if covalency becomes dominant—which could be true at sufficiently small ion separations. Consequently, all superposition model investigations only using the monotonic expansion (10) to represent $\bar{b}_2(r)$ at iron-ligand spacings less than about 1.9 Å should be viewed with some skepticism.

Thus, different from Zhou Yi-Yang[4] and Zheng Wen-Chen[5] we include the Lennard-Jones type expression in our superposition model analysis, which we will present below. But before doing so, it seems reasonable to summarize a few further comments on the assumptions made *a priori* in applying the superposition model.

(1) Independence of $\bar{b}_2(r)$ of the coordination number of the defect ion. Although this proposition makes the superposition model a very powerful tool for interpretations of axial EPR parameters of S-state ions, its range of validity is not quite clear. Indeed, theoretical investigations (e.g., Refs. 12, 14, and 15) emphasize the importance of covalency between the defect and its ligands for the above-mentioned EPR parameters. It is seen that these parameters depend to a considerable extent on overlap and charge transfer coefficients, which are part of the quantum-mechanical state function of the defect complex. If these coefficients are treated as variational parameters they should, in principle, reflect possible changes in the defect geometry.

(2) Independence of $\bar{b}_2(r)$ of charge and size misfit of the defect ion. Assumptions of this kind are certainly of limited validity, as has been demonstrated by the careful investigations of Müller and Berlinger.[13] These authors emphasize that charge and size misfits of the impurity ion significantly change the local strain-coupling coefficients around the defect, from which the $\bar{b}_2(r)$ parameters are derived. For the case of Fe^{3+} Müller and Berlinger suggest to reduce the absolute value of $\bar{b}_2(R_0)$ by at least 11% of its initial value for each positive unit of charge misfit (i.e., 22% for Fe_K^{3+}).

(3) Generally the size of defect-induced relaxations is not restricted. However, it is reasonable to consider such restrictions based at least on ion-size arguments in order to exclude artificial solutions.

The discussion given above may suffice to demonstrate that superposition model investigations should be viewed critically, if one has to expect considerable deviations of the environment with respect to the original geometry for which the $\bar{b}_2(r)$ function was derived. This certainly concerns the Fe_K^{3+} related problems (e.g., Fe_K^{3+} in $KTaO_3$ has twelve O^{2-} neighbors as compared to six in the standard case MgO:Fe^{3+}). We therefore only derive conclusions from qualitative differences in the $\bar{b}_2(r)$ functions (9) and (10) since their exact functional dependence is not known over the entire range of possible separations.

This critical point of view towards the superposition model in this special case is one reason for us to use shell-model calculations as an independent approach to find some support for our superposition-model results.

The crystal lattice responds to the substitution of iron at the potassium site by relaxation. In order to keep the number of variables small our calculations are based on a simplified treatment of the relaxation of the oxygen ligands. The 12 oxygens surrounding the potassium site are divided among three planes perpendicular to the axial direction of the defect center. The displacements of the oxygen ions are confined to these planes, i.e., the movements in the upper and lower plane are along [1,0,0]-type directions and in the central plane along [1,1,0]-type directions (Fig. 1). The movement was parametrized by the distance of the oxygens from their original positions.

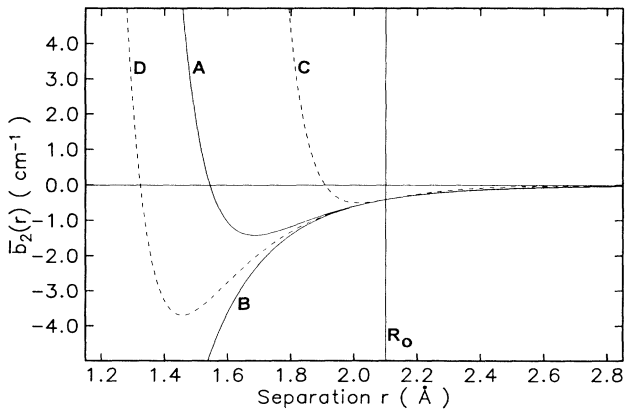

FIG. 2. Different $\bar{b}_2(r)$ functions. (a) Lennard-Jones function, Eq. (9); (b) inverse power-law function equation (10); (c) and (d) Lennard-Jones functions.

Such relaxations have also been included in the approach of Zhou Yi-Yang.[4] We find that the results remain qualitatively unaltered when different choices of relaxation are made.

In addition we have considered different off-center displacements of Fe^{3+} along the z axis. All these calculations were performed for both $\bar{b}_2(r)$ dependences, (9) and (10), and for isolated Fe_K^{3+} as well as for Fe_K^{3+}-O_I. The local geometry is therefore given by the distance of the oxygen ions from their original positions and the off-center coordinate of the iron defect. Figure 1 shows the site assumed for possible oxygen interstitial ions.

In the case of an oxygen interstitial being present, its position was fixed on the z axis. Several runs were made with different positions in order to check this dependence. The geometrical configurations that yield the experimental value of $D=4.46$ cm^{-1} are shown in Figs. 3 and 4. In the calculations on which these figures are based an oxygen interstitial was present at a fixed position 1 Å below the central oxygen plane.

Figure 3 shows the solutions in the case of the monotonic $\bar{b}_2(r)$ function (10). In order to reproduce the measured D value a relaxation of the oxygen ligands of at least 0.32 Å towards the z axis is required. A displacement of the Fe^{3+} of approximately 2.00 Å along the z axis corresponds to this oxygen displacement.

For such solutions the effect of a possible oxygen interstitial can be neglected because of its large distance from Fe^{3+}. Two important points should now be noted. Firstly, because of ion size arguments oxygen relaxations (such as specified in this section) which significantly exceed 0.3 Å should be ruled out, otherwise there would be strong overlap repulsion between the oxygen ions. Already an oxygen relaxation of 0.3 Å leads to oxygen-oxygen separations of 2.4 Å (this value is to be compared with twice the oxygen radius 2.5–2.8 Å). Secondly, in neither of the defect cases, isolated Fe_K^{3+} or Fe_K^{3+}-O_I, do we find a plausible explanation for the large Fe_K^{3+} off-center displacement.

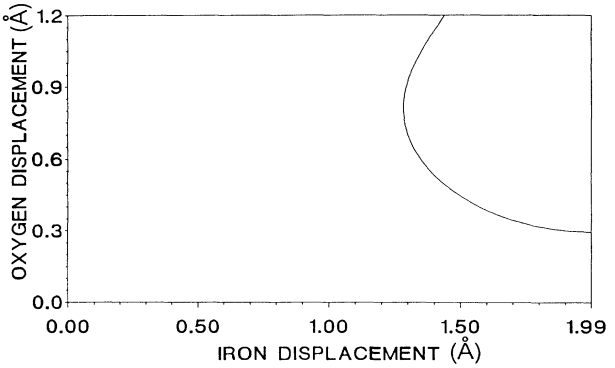

FIG. 3. Geometrical configurations which yield the experimental value for $D=4.46$ cm^{-1} using the inverse power-law $\bar{b}_2(r)$ function (10). An oxygen interstitial ion was positioned at 1 Å below the central oxygen plane. The iron displacement starting in the central oxygen plane is along the z axis towards the upper plane. The oxygen ligand ions are displaced towards the z axis within their respective planes.

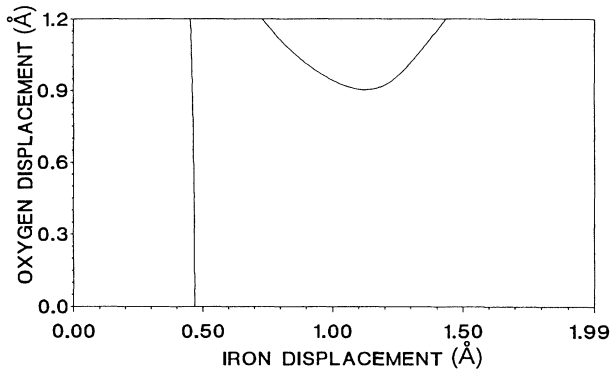

FIG. 4. Geometrical configurations which yield the experimental value for $D=4.46$ cm^{-1} using the Lennard-Jones-type $\bar{b}_2(r)$ function (9). An oxygen interstitial ion was positioned at 1 Å below the central oxygen plane. The assignment of displacements is as given in Fig. 3.

There are other solutions that require less off-center displacement of the iron, but these lead to an even larger contraction of the oxygens surrounding the defect. Moreover, if we include corrections resulting from misfit effects, i.e., reduction of the absolute value of $\bar{b}_2(R_0)$ by about 22%, one comes up with even more unrealistic oxygen relaxations in order to explain the observed D value. In addition we note that large iron and oxygen relaxations are ruled out on the basis of our shell model calculations, too (Sec. II). In summary the solutions in Fig. 3 correspond to rather unphysical relaxations.

If a superposition model analysis is performed using the Lennard-Jones function (9) instead of (10), we find that the $[Fe^{3+}$-$O_I]$ defect complex together with moderate oxygen ligand relaxations is the only physically reasonable solution. The straight line in Fig. 4 corresponds to this solution. The curved part in Fig. 4 belongs to solutions based on large oxygen ligand relaxations, which are physically unreasonable. Calculations with the radial function (10) yield the correct D value for a Fe_K^{3+}-O_I distance of $\simeq 1.5$ Å. This can clearly be seen from Fig. 4 where the line indicates the correct solution for an iron off-center shift of just under 0.5 Å. To this the distance of the interstitial oxygen from the central oxygen plane of 1.0 Å (fixed) has to be added. Shifting the position of the oxygen interstitial results in a parallel shift of the straight line in Fig. 4 leading to the same distance between Fe_K^{3+}-O_I of $\simeq 1.5$ Å in every case.

We emphasize that our superposition-model analysis given so far can only give some useful qualitative hints, because of the well-known problems with $\bar{b}_2(r)$ functions which were discussed above and because of the possible limitations of the superposition model itself in this special case.

Thus we do not attempt to interpret the calculated Fe_K^{3+}-O_I distance of $\simeq 1.5$ Å as being significant, but, far more, we invoke the principle occurrence of a physically satisfactory solution if one is using the Lennard-Jones-type function. In Fig. 2 we have also included certain limiting Lennard-Jones-type $\bar{b}_2(r)$ functions, which agree

with the dependences given above at R_0 but show up significant deviations at smaller r values (dotted curves). In particular it is noted that the dotted curve C in Fig. 2 would be consistent with our shell-model results.

IV. SUMMARY

We have investigated the incorporation of Fe^{3+} ions in $KTaO_3$ by means of a computer simulation based on the shell model. In general such calculations are very useful to elucidate the chemically most favorable defect structures in ionic or semi-ionic materials as well as type and magnitude of defect-induced lattice relaxations.

In the present simulation study it could be shown that Fe^{3+} ions enter $KTaO_3$ by substituting ions of both cation species, i.e., Fe_{Ta}^{3+} defects are charge compensated by formation of an equal number of Fe_K^{3+} defects. The latter defect species is usually invisible in EPR experiments if no precautions are made to correct for the reducing growth conditions of $KTaO_3$ crystals. Experiments show that codoping $KTaO_3$ with Ti^{4+} results in observable cubic Fe^{3+} centers. This is consistent with the result from shell-model simulations.

Moreover, we find the formation of oxygen Frenkel-defect pairs to be energetically feasible if the oxygen defects are bound to Fe^{3+} centers. This mechanism then provides a natural source for $[Fe_{Ta}^{3+}\text{-}V_0]$ and $[Fe_K^{3+}\text{-}O_I]$ defect complexes, which can be related to the two experimentally known axial EPR centers. In particular the large axial EPR parameter $D=4.46\ cm^{-1}$ is explained by $[Fe_K^{3+}\text{-}O_I^{2-}]$ defect complexes.

We note that all defect-induced lattice relaxations in the cases under investigation are of moderate size (less than ≈ 0.30 Å)—in agreement with ion size arguments. Especially, they are not sufficient to provide an explanation for the observed large D parameter for the axial Fe_K^{3+} center, as was recently assumed in a superposition model analysis by Zhou Yi-Yang. Using a simple inverse power law for the occurring $\bar{b}_2$ radial function he found a nearby oxygen interstitial to give a negative contribution to the D parameter and thus concluded that charge compensation is made by a remote oxygen interstitial and that relaxation effects are dominant.

In our superposition model analysis we use instead a Lennard-Jones-type $\bar{b}_2$ radial function, as proposed by Newman, which is physically more reasonable than the inverse power law. In this approach the contribution of a nearby oxygen interstitial ion is positive and large relaxation effects do not have to be considered in order to produce the large D parameter.

The $[Fe_K^{3+}\text{-}O_I^{2-}]$ defect center is responsible for the observed large value of the axial zero-field splitting parameter D in EPR experiments. The result is explained by properties of the defect pair itself and not by ligand relaxations.

ACKNOWLEDGMENTS

We wish to thank Professor O. F. Schirmer for useful discussions throughout the course of this work. This study was supported by Deutsche Forschungsgemeinschaft (DFG), Sonderforschungsbereich 225.

[1]D. M. Hannon, Phys. Rev. **164**, 366 (1967).
[2]I. P. Bykov, M. G. Glinchuk, A. A. Karmazin, and V. V. Laguta, Fiz. Tverd. Tela **25**, 3586 (1983) [Sov. Phys. Solid State **25**, 2063 (1983)].
[3]E. Siegel and K. A. Müller, Phys. Rev. B **19**, 109 (1979).
[4]Zhou Yi-Yang, Phys. Rev. B **42**, 917 (1990).
[5]Zheng Wen-Chen, Phys. Rev. B **45**, 3156 (1992).
[6]B. G. Dick and A. W. Overhauser, Phys. Rev. **112**, 90 (1958).
[7]*Computer Modelling of Solids,* Springer Lecture Notes in Physics Vol. 166, edited by C. R. A. Catlow and W. C. Mackrodt (Springer, Berlin, 1982).
[8]G. V. Lewis and C. R. A. Catlow, J. Phys. Chem. Solids **47**, 89 (1986).
[9]M. Exner, H. Donnerberg, O. F. Schirmer, and C. R. A. Catlow (unpublished).
[10]H. Donnerberg, S. M. Tomlinson, C. R. A. Catlow, and O. F. Schirmer, Phys. Rev. B **44**, 4877 (1991).
[11]D. J. Newman, Adv. Phys. **20**, 197 (1971).
[12]D. J. Newman and W. Urban, Adv. Phys. **24**, 793 (1975).
[13]K. A. Müller and W. Berlinger, J. Phys. C **16**, 6861 (1983).
[14]P. Novak and I. Veltrusky, Phys. Stat. Sol. **73**, 575 (1976).
[15]M. Heming, S. Remme, and G. Lehmann, Ber. Bunsenges. Phys. Chem. **88**, 946 (1984).